Carbohydrate Polymers 90 (2012) 8–15

Contents lists available at SciVerse ScienceDirect

Carbohydrate Polymers

journal homepage: www.elsevier.com/locate/carbpol

Fast and long-acting antibacterial properties of chitosan-Ag/polyvinylpyrrolidone nanocomposite films

Bai-Liang Wang, Xiang-Sheng Liu, Ying Ji, Ke-Feng Ren, Jian Ji*

MOE Key Laboratory of Macromolecule Synthesis and functionalization, Department of Polymer Science and Engineering, Zhejiang University, Hangzhou 310027, China

ARTICLE INFO

Article history:
Received 16 December 2011
Received in revised form 22 March 2012
Accepted 24 March 2012
Available online 1 April 2012

Keywords:
Silver nanoparticles
Chitosan
Polyvinylpyrrolidone
Nanocomposite films
Antibacterial
Medical devices

ABSTRACT

Infection associated with medical devices is one of the most frequent complications of modern medical biomaterials. Preparation of antibacterial films on the medical devices is a great challenge owing to bactericidal efficiency, long acting and biocompatibility. In this study, silver nanoparticles (Ag NPs) doped chitosan/polyvinylpyrrolidone (PVP) films were successfully prepared by dip coating method. The nanocomposite films with spherical Ag NPs (diameters in 10–50 nm) were stable after being immersed in PBS for 35 days. Through regulating the concentration of $AgNO_3$, the nanocomposite films showed good cell compatibility. The nanocomposite films could eliminate 100% *Staphylococcus aureus* (ATCC 6538) and *Escherichia coli* (ATCC 8739) in 5 min and had favorable long-acting antibacterial property. The increase of PVP amount obviously enhanced anti-adhesion activity of the nanocomposite film. Such nanocomposite films can be expected to have good potential in biomaterials applications.

1. Introduction

Medical devices-related infections present serious ongoing problems in the biomedical field. Surface modification of the medical devices can obviously reduce the incidence of infections. There are mainly three strategies for the antibacterial surface design (Lichter, Van Vliet, & Rubner, 2009): anti-adhesion surface, contact killing surface and biocide agent leaching surface. However, anti-adhesion surface can hardly last a long time. Contact killing surface with admirable bactericidal activity always has certain cytotoxicity towards mammalian cell and cannot release bacteria corpse which is easy for bacteria adhesion. For the third antibacterial surface, the release of biocide agent is not easy to adjust and control. A composite film with multiple antibacterial properties may offset the shortcomings of the above three antibacterial surfaces.

Chitosan is hydrophilic, atoxic, biodegradable, biocompatible and cationic: it exerts either bacteriostatic or bactericidal activity by disrupting the inner organelles or disturbing the metabolism of certain bacterial strains (Muzzarelli et al., 1990, 2012). Due to the strong inter- and intra-molecules hydrogen bondings between chitosan chains, it can easily form a stable film. Unfortunately, chitosan promotes plasma protein adsorption, platelet adhesion and activation, and thrombus development, which is appropriate for bacteria adhesion (Lord, Cheng, McCarthy, Jung, & Whitelock, 2011). In order to overcome the disadvantages, chitosan has been combined with carrageenan (Bratskaya et al., 2007), hyaluronic acid (Yamane et al., 2005), polyethylene glycol (Li, Zivanovic, Davidson, & Kit, 2011), heparin, or sodium alginate (Han, Zhou, Yin, Yang, & Nie, 2010) to enhance its anti-adhesion properties. In our previous works, through combining with a hydrophilic polymer, a $(chitosan/heparin)_n$ multilayer film through layer-by-layer self-assembly method with both anti-adhesive and antibacterial properties was obtained (Fu, Ji, Yuan, & Shen, 2005). Furthermore, a composite film of $(chitosan\text{-}Ag/heparin)_n$ multilayer film was prepared, which were effective in killing *Escherichia coli* and had low cell toxicity. However, the method needs intermediate washing and drying steps, which is a time consuming and complicated operation (Fu et al., 2006).

Silver has long been known to have broad and strong antibacterial activity (Kang, Jung, & Jeong, 2000). Silver nanoparticles (Ag NPs) can delay the release of silver ions to act a long-acting antibacterial property. Firstly, silver ions can be incorporated into solid films either by immersion of the films with ion-binding groups (such as amino groups) into silver ions solution or by self-assembly of silver ions with polymer template in solution before film formation. Subsequently, in situ reduction of silver ions can produce Ag NPs (Lala et al., 2007). The advantages of this method to obtain Ag NPs are its ease of preparation, convenience in use, and uniform in shape and size. Although a broad antibacterial effect, silver ions with high concentration possess cytotoxicity. Through

* Corresponding author. Tel.: +86 571 87953729; fax: +86 571 87953729.
E-mail address: jijian@zju.edu.cn (J. Ji).

0144-8617/$ – see front matter © 2012 Elsevier Ltd. All rights reserved.
http://dx.doi.org/10.1016/j.carbpol.2012.03.080

regulating amount of incorporated Ag NPs and release behavior of silver ions, the issue of cytotoxicity may be well solved. Polyvinylpyrrolidone (PVP) has attracted considerable interest due to its hydrophilicity, lubricity, anti-adhesive property and excellent biocompatibility. Moreover, PVP and chitosan can form a homogeneous phase due to the strong hydrogen binding forces between two kinds of molecules (Anjali Devi, Smitha, Sridhar, & Aminabhavi, 2006; Sakurai, Maegawa, & Takahashi, 2000; Smitha, Sridhar, & Khan, 2006). Chitosan as an effective bactericidal polycation natural macromolecule can be used as template for Ag NPs preparation (Yang, Wang, Huang, & Hon, 2010) and form a homogeneous miscible solution with PVP (Cao, Shi, & Chen, 1998).

In this study, chitosan-Ag/PVP nanocomposite films were prepared by a dip coating method. Surface morphology, wettability and stability of the films were measured. The formation of Ag NPs was observed by UV–visible spectrum and transmission electron microscopy. Morphology and activity evaluation of endothelial cells were used to explore the cell compatibility of the films. Bactericidal activity, anti-adhesion activity and long-acting bactericidal activity were measured respectively with *E. coli* and *S. aureus* as model bacteria. The achievement of the chitosan-Ag/PVP nanocomposite films with anti-adhesion, fast and long-acting multifunctional antibacterial properties can potentially be wide used on surface modifications of biomaterials.

2. Materials and methods

2.1. Materials

Chitosan (K2210, viscosity: 55 cps, degree of deacetylation is 92%) used in this work was obtained from Sanland-chem international Inc. Polyvinylpyrrolidone (PVP) (*K* value: 29–32), polyetherimide (PEI) (M_w: 25 kDa) and polyacrylic acid (PAA) (35 wt%, M_w: 10 kDa) were purchased from Sigma–Aldrich. $AgNO_3$ was purchased from Sinopharm Chemical. PET sheet was purchased from Hangzhou Magnetic Tape Corporation of China. Trypicase soy agar (TSA) and Trypicase soy broth (TSB) were purchased from Hangzhou Baisi Corporation of China. *Staphylococcus aureus* (*S. aureus*) (ATCC 6538) and *Escherichia coli* (*E. coli*) (ATCC 8739) were kindly provided by Prof. Jian Xu (Zhejiang University, Hangzhou, China). Ultrapure distilled water was obtained after purification using a Millipore Milli-Q system (USA).

2.2. Clean and pretreatment of substrates

After cutting into certain shape ($3 \times 2\,cm^2$), PET sheets were successively cleaned in ethanol, acetone and water for 10 min respectively, and then dried with N_2. Silicon wafers ($1 \times 2\,cm^2$) were cleaned in sulfuric acid/hydrogen peroxide bath (piranha) and were used for film thickness and surface morphology measurement in field emission scanning electron microscope (FE-SEM) due to their brittle fracture property. Then PET sheets and silicon wafers were successively immersed in PEI solution (5 mg/ml, 30 min) (Boulmedais et al., 2004), PAA solution (5 mg/ml, 30 min) and 1-Ethyl-3-(3-dimethylaminopropyl) carbodiimide (EDC)/N-hydroxysulfosuccinimide (sulfo-NHS) solution (EDC: 10 mmol, sulfo-NHS: 20 mmol, 12 h) at 25 °C.

2.3. Preparation of chitosan-Ag/PVP nanocomposite films

For the preparation of chitosan-Ag/PVP nanocomposite films, $AgNO_3$ (0.05–1 mmol), PVP (wt% = 0%, 15%, 25%, 35%, 50%) and chitosan (1 wt%) were successively added into HAc/NaAc buffer (0.1 M, pH = 4.0) with magnetic stirring for 2 h. Dip coating method was used to prepare chitosan-Ag/PVP films on the pretreated PET sheets and silicon wafers. The nanocomposite films were dried at 25 °C for 24 h and for 12 h under vacuum at 30 °C. Then Ag NPs were obtained through thermal reduction at 110 °C for 4 h (Clemenson, David, & Espuche, 2007; Mahltig et al., 2009). Silver ions were initially coordinated with hydroxy groups and amino groups of chitosan to form a chelate structure. In the process of thermal treatment, hydroxy groups and amino groups of chitosan acted as reductive agents to generate Ag NPs. Color change of the films from transparent to brown indicated the formation of Ag NPs.

2.4. Characterization of the films

Surface morphology was measured by atomic force microscope (AFM, SPA 400, Seiko instrument Inc.). AFM images were performed in the tapping mode under ambient conditions using a commercial scanning probe microscope, equipped with a silicon cantilever, nanosensors, typical spring constant 40 N m^{-1}. Surface wettability of the films was measured by Drop Shape Analysis (KRŰSS, DSA10-MK2). The sessile dropping method was used to detect surface of the film within 15 s after the water droplet contacted the film. FE-SEM (FEI, SiRion100) was carried out to measure film thickness and surface morphology on silicon wafers instead of PET sheets. UV–visible spectrum was recorded on a UV–visible spectrophotometer (CARY100 BIO, America). For transmission electron microscopy (TEM) imaging, the nanocomposite films were immersed in hydrofluoric acid solution and the films instantly broke off from the PET substrates. The solutions were immediately picked up with copper TEM grids and were blown dried gently. TEM was performed with a JEOL JEM-1230FX operated at either 100 or 200 kV. The amounts of silver ions released and total silver loaded in the nanocomposite film were measured by inductively coupled plasma mass spectrometry (ICP-MS, XSeries II, Thermo Elemental Corporation of USA) after Ag NPs dissolving in 1.0 M HNO_3.

2.5. In vitro antibacterial test

Antimicrobial tests of chitosan-Ag/PVP nanocomposite films were conducted qualitatively and quantitatively by shake-flask culture method, waterborne antiadhesion test and zone inhibition method respectively with *E. coli* (ATCC 8739) and *S. aureus* (ATCC 6538) as model bacteria.

For shake-flask culture method, chitosan-Ag/PVP nanocomposite films coated PET sheets were placed in test tubes with 10 ml 1.1×10^5 cells/ml of initial *E. coli* (or *S. auresus*) suspension in PBS. These tubes were shaken at 200 rpm in incubators at a constant temperature of 37 °C. At predetermined time, bacteria suspensions were pipetted out from the tubes, and consecutive dilutions were prepared by taking 0.1 ml of the previous solution and mixed with 9.9 ml of PBS. From the solution, 0.2 ml was plated onto the triplicate solid agar using the spread plate method. After incubating for 24 h, the number of viable bacteria was counted and the results were expressed as mean colony forming units (CFU) per ml. The survival ratio of bacteria was defined as the percentage of viable bacteria in the suspension relative to the total number of the initial bacteria in the suspension. Results represent mean ± SD of triplicates from three separate experiments ($P < 0.05$).

For the waterborne assay, chitosan-Ag/PVP nanocomposite films coated on PET sheets were immersed into sterile plastic tubes with 10 ml 1.1×10^7 cells/ml initial bacteria suspensions in PBS and these tubes were shaken at 200 rpm at 37 °C for 4 h. The films were then removed and washed gently three times with sterile PBS and immersed into 3 vol% glutaraldehyde solution in PBS at 4 °C for 4 h. The glutaraldehyde solution was then removed and the films were washed with PBS, followed by dehydration with 25, 50, 70, 95 and 100 vol% ethanol for 10 min each. The films were then dried and sputter-coated with a thin film of gold for imaging purposes. The films after waterborne tests were characterized by SEM.

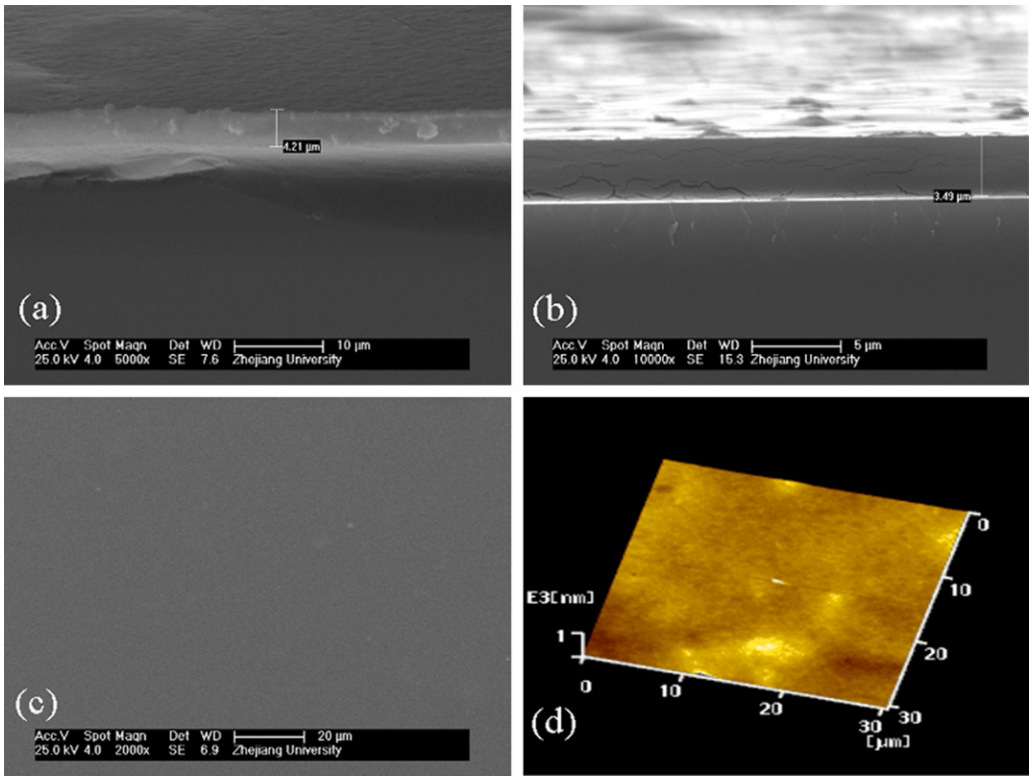

Fig. 1. SEM images of cross-section (a) before and (b) after being immersed in PBS for 35 days and (c) surface morphology and (d) AFM images of chitosan-Ag/PVP nanocomposite film with 0.25 mmol $AgNO_3$ added.

Zone inhibition test was carried out with a modified agar diffusion assay. Chitosan-Ag/PVP films coated on PET sheets were placed on nutrient agar in Petri dishes which had been seeded with 0.2 ml of 1.1×10^5 cells/ml bacteria suspension. The Petri dishes were examined for zone of inhibition after 24 h incubation at 37 °C. The area clearing surrounded the film where bacteria were not capable of growing was reported as the zone of inhibition.

2.6. In vitro cytotoxicity test

The human umbilical vein endothelial cells (HUVECs) were used to evaluate cell toxicity by cell morphology evaluation and cell activity test (Bancel & Hu, 1996Bancel, & Hu, 1996). The HUVECs were maintained in RPMI.1640 supplemented with 10% heat-inactivated (30 min, 56 °C) fetal bovine serum (Sijiqin Biotech, China, lot no.020613.2), 100 units/ml penicillin, 100 μg/ml streptomycin 50 μg/ml gentamicin (Gibco) and kept at 37 °C in a humidified 5% CO_2 atmosphere. Chitosan-Ag/PVP nanocomposite films modified PET sheets, sterilized in 75% ethanol and swollen in PBS, were placed into 96-well tissue culturing polystyrene (TCPS) plates (NUCLONTM, Cat. No.167008). The HUVECs were then seeded in culture media to give a final density of 1×10^4 cells/well and incubated for 24 h at 37 °C in an atmosphere of 5% CO_2 in air. Cell activity was determined by 3-(4,5-cimethylthiazol-2-yl)-2,5-diphenyl tetrazolium bromide (MTT) assay. The absorbance values were measured by using microplate reader (Bio-Rad, model 550) at wavelength 570 nm, blanked with dimethyl sulfoxide (DMSO) solution. Five replicates were read for each sample, the mean value of the five was used as the final result.

The cell monolayers on surfaces of chitosan-Ag/PVP nanocomposite films were also stained with fluorescein diacetate (FDA, Sigma) for fluorescence microscope investigation (Olympus DP71 microscope at 20× magnification in fluorescein filter, 488 nm excitation). FDA is an indicator of membrane integrity and cytoplasmic esterase activity. Stock solutions were prepared by dissolving 5.0 mg/ml FDA in acetone. The working solution was freshly prepared by adding 50 μl of FDA stock solution into 5.0 ml of PBS. FDA solution (20 μl) was added into each well and incubated for 5 min. The films were then washed twice with PBS and placed on a glass slide for fluorescence microscope examination. Cells incubated into wells that did not contain materials were used as controls.

3. Results and discussion

3.1. Preparation of chitosan-Ag/PVP nanocomposite films

3.1.1. Stability and surface morphology

Stability of the film imposes restrictions on its application. Chitosan-Ag/PVP nanocomposite films were prepared by dip coating method. As can be observed in Fig. 1a, a uniform and firmly binding film formed on the silicon wafer with thickness of ~4 μm. The feeds of PVP and $AgNO_3$ in the chitosan-Ag/PVP film for SEM test were 25 wt% and 1 mmol. Chitosan possesses high swelling capacity and PVP is a high hydrophilic polymer. Thus, and the nanocomposite films could be easily detached from the supports when immersed in water environment with lots of blisters forming between the nanocomposite films and the supports (date not shown). The similar phenomenon has been reported in other article (Picart et al., 2005). Pretreatment of supports by PEI, PAA and EDC/sulfo-NHS greatly enhanced binding ability of the nanocomposite films on the surface of substrates. Substrate modified by PEI as a precursor layer which was rich in amino group. PAA with carboxyl group and PEI with amino group were cross-linked by EDC/suflo-NHS and the unreacted carboxyl group of PAA could further react with amino group of chitosan (Richert et al., 2004; Susumu et al., 2007). SEM section image was used to investigate the thickness changes of chitosan-Ag/PVP nanocomposite films before and after being immersed in PBS for 35 days. As illustrated in Fig. 1b,

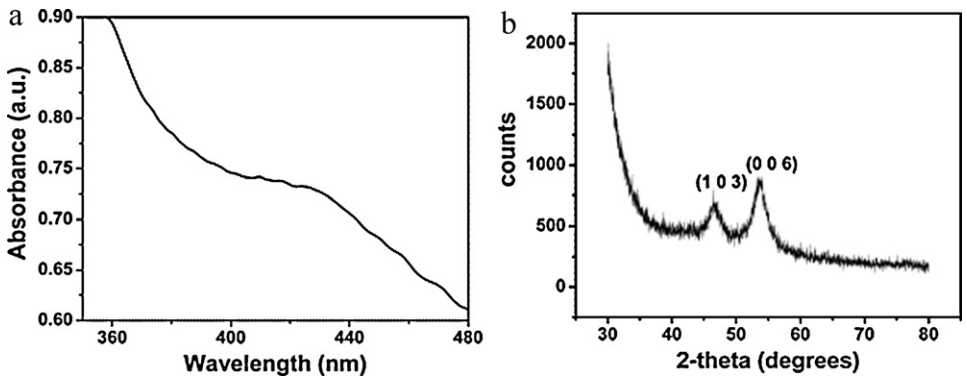

Fig. 2. (a) UV–visible spectra and (b) X-ray diffractogram of chitosan-Ag/PVP nanocomposite film with 1 mmol $AgNO_3$ added.

after immersing, the nanocomposite film still firmly integrated with silicon wafers and the thickness was uniform. The loss of only about 10% of thickness indicated that the silver-loaded nanocomposite films had a good stability.

The surface morphology of the nanocomposite film was investigated by SEM and AFM. As indicated in Fig. 1c, the surface of the film was flat and smooth, which is beneficial to resist bacteria adhesion (Teixeira et al., 2006). As shown in Fig. 1d, the 3D AFM image clearly illustrated the number and height of the peaks on the surface of the chitosan-Ag/PVP nanocomposite film with 25 wt% PVP and 0.25 mmol $AgNO_3$ added. The RMS roughness ($30 \times 30\,\mu m^2$) was 13.3 ± 1.7 nm for the chitosan-Ag/PVP nanocomposite films with 25 wt% PVP and 0.25 mmol $AgNO_3$ and showed no obvious difference with different amount of $AgNO_3$ in the films. Chitosan and PVP could form a homogeneous phase construction through strong inter- and intra-molecular hydrogen bondings. The addition of the small amount of $AgNO_3$ added had little effect on the construction of the films.

3.1.2. Characterization of Ag NPs

The incorporated Ag NPs in the films were obtained by thermal reduction method with hydroxy groups and amino groups of chitosan as reductant groups. The UV–visible spectrum of the chitosan-Ag/PVP nanocomposite films after thermal reduction at 110 °C for 4 h was recorded and presented in Fig. 2a. As the input $AgNO_3$ concentration in the film was so low that a weak superimposed broad band intensity appeared and there was no obvious absorption peak when the $AgNO_3$ concentration input was lower than 1 mmol (date not shown). A fairly broad resonance centered at ca. 425 nm was observed and it clearly indicated the presence of polydispersity Ag NPs in the chitosan/PVP matrix (El-Rafie, Mohamed, Shaheen, & Hebeish, 2010). It is well known that Ag NPs exhibit absorption in the UV–visible region due to their characteristic surface plasmon resonance frequency. The crystallinity of the formed Ag NPs in the films was assessed by XRD analysis. Fig. 2b showed the XRD spectra of the nanocomposite film. The presence of two broad bands with strong peaks centered

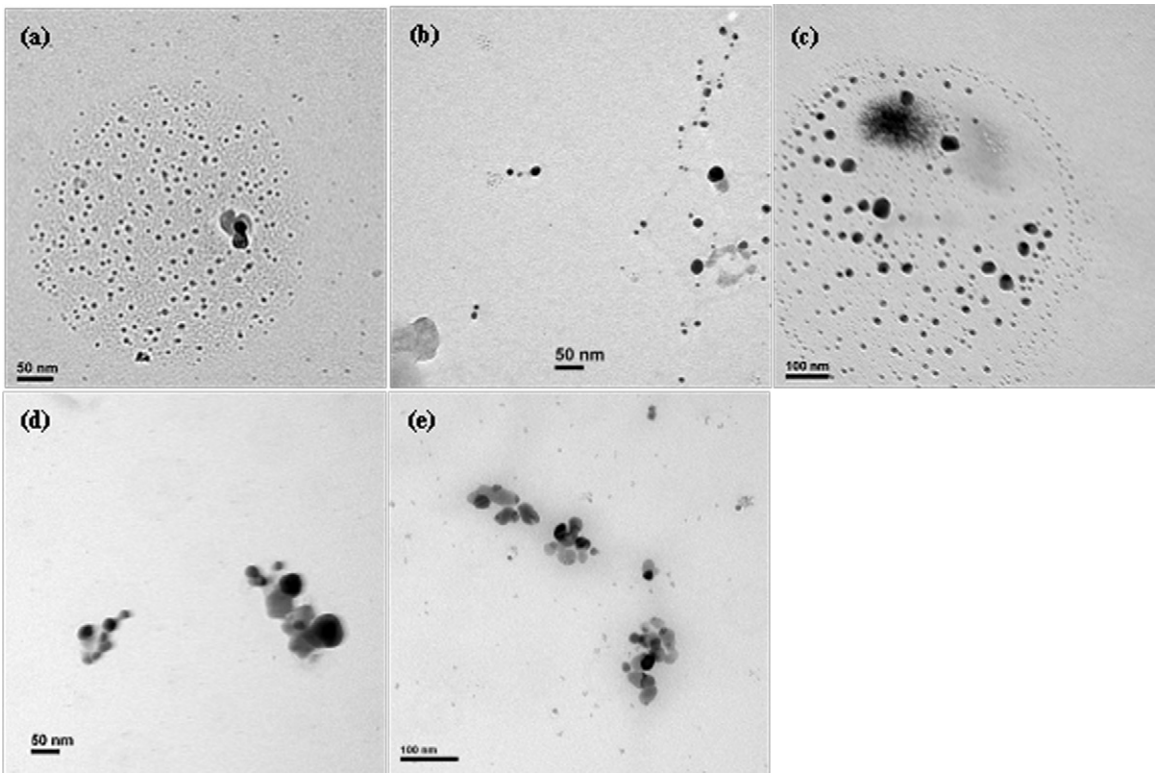

Fig. 3. TEM images of chitosan-Ag/PVP nanocomposite film with different feeds of $AgNO_3$: (a) 0.05 mmol, (b) 0.1 mmol, (c) 0.25 mmol, (d) 0.50 mmol, and (e) 0.75 mmol.

in $2\theta = 46.4^\circ$ and $2\theta = 53.5^\circ$ could be assigned to the (1 0 3) and (0 0 6) planes of hexagonal Ag NPs (standard cards No. 00-041-1402). The intense peaks indicated that highly crystalline silver nanostructures formed in the chitosan-Ag/PVP nanocomposite film.

Chitosan-Ag/PVP nanocomposite film was subjected to TEM with a view to explore the size, shape and distribution of Ag NPs. Fig. 3 depicted TEM images of Ag NPs with different amount of $AgNO_3$ added to chitosan-Ag/PVP nanocomposite films. It could be observed that spherical Ag NPs formed after thermal reduction process. Chitosan and PVP were both stabilizers for Ag NPs formation (Tolaymat et al., 2010). The more $AgNO_3$ was added, the larger the diameter of Ag NPs was obtained. The diameters of Ag NPs ranged from 10 nm to 20 nm for 0.05 mmol $AgNO_3$ nanocomposite film to 30–50 nm for 0.75 mmol $AgNO_3$ nanocomposite film. It suggested that the size and the loading amount of Ag NPs could be controlled by adjusting the concentration of silver ions in the dip coating solution. Therefore, it is possible to tune the release of silver ions by controlling the size of Ag NPs. Furthermore, Ag NPs prepared with higher concentration of $AgNO_3$ had a stronger tendency to aggregate.

3.1.3. Release of silver ions

In order to explore the release behaviour of the chitosan-Ag/PVP (0.25 mmol $AgNO_3$) nanocomposite film, the film was immersed in 30 ml PBS with medium change at predetermined time. Silver ions concentration was measured by ICP-MS. As indicated in Fig. 4, there was a burst release process in the first day with 21.12 ± 2.36 ppm at 30 min and 38.63 ± 2.65 ppm at 3 h. Then the nanocomposite film slowly released silver ions at a rate of 0.58–2.04 ppm per day for the next 26 days. Such concentration was much higher than the minimal inhibitory concentration of Ag^+ (0.12 ppm) (Chen & Wu, 2005Chen et al., 2005). The total silver amount of 245.76 ± 26.93 μg of the film was measured by dissolving silver ions in HNO_3 and tested by ICP-MS. Comparing with other Ag NPs loading coatings (Rhim, Hong, Park, & Perry, 2006) the chitosan-Ag/PVP nanocomposite film could obviously delay the release speed of silver ions. At such a speed, the release of silver ions from the nanocomposite film will last a longer time and exhibit effective antibacterial properties.

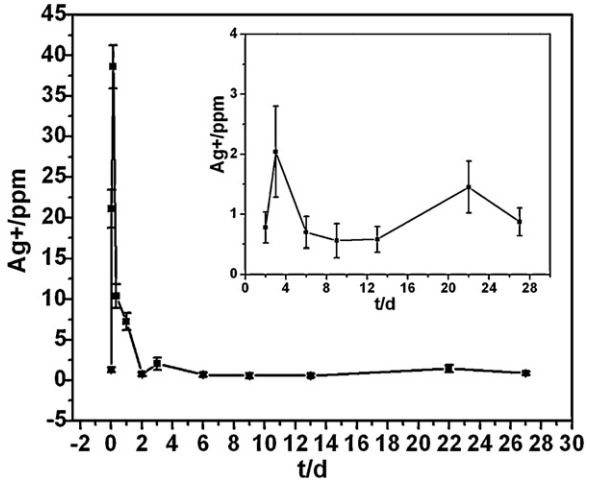

Fig. 4. Release of Ag ions from chitosan-Ag/PVP (0.25 mmol $AgNO_3$) nanocomposite film tested by ICP-MS.

3.2. In vitro cytotoxicity tests

High concentration of silver ions possesses severe cytotoxicity. Through regulating the amount of incorporated Ag NPs, the issue of cytotoxicity may be well solved. Human umbilical vein endothelial cells (HUVECs) were used to test the cytotoxicity by cell morphology and activity evaluation with PET sheets, chitosan/PVP film and TCPS as negative controls. Fig. 5 showed the cell activity of HUVECs on various surfaces over a period of 24 h. According to Fig. 5, the surfaces of PET, TCPS and chitosan/PVP film were good for HUVECs growth and proliferation. With the increase of added $AgNO_3$, more Ag NPs formed in the films. Consequently, the cell amount on the nanocomposite films gradually decreased and the cells could not maintain normal spreading morphology.

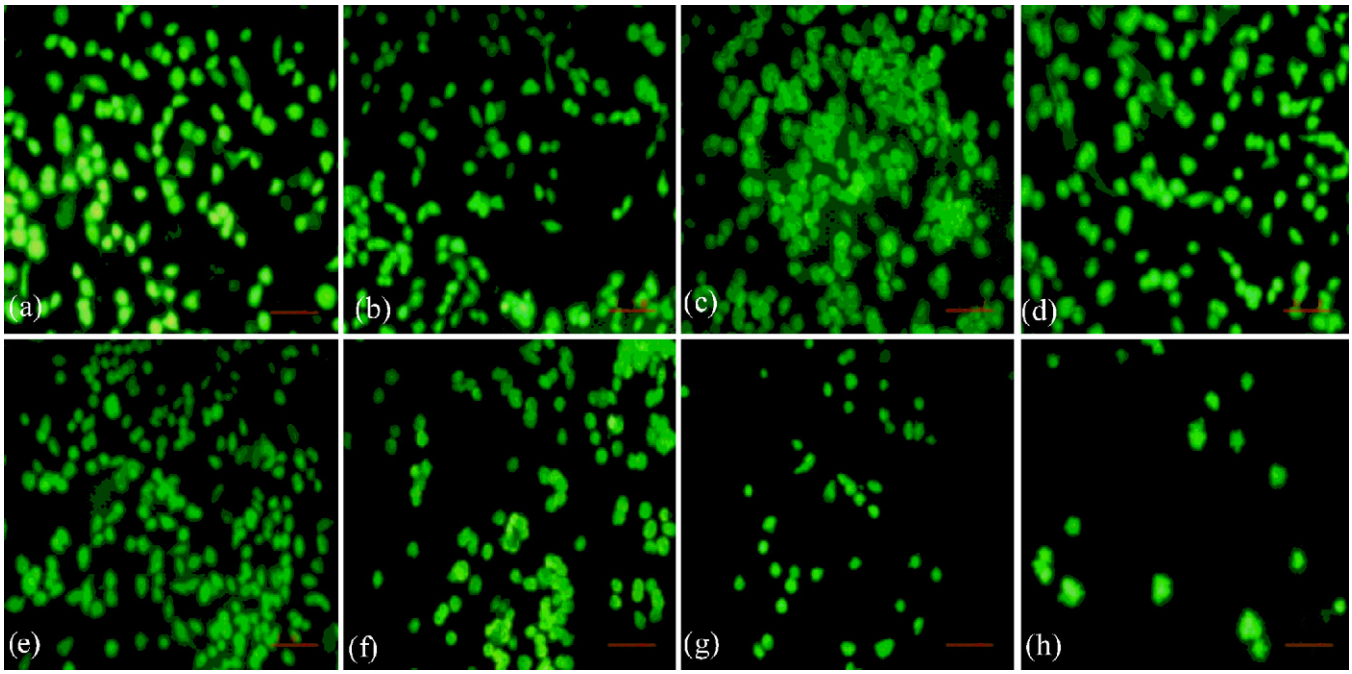

Fig. 5. Fluorescence microscope images of HUVECs on (a) TCPS, (b) pristine PET sheet, (c) chitosan/PVP film, and chitosan-Ag/PVP nanocomposite films with different feeds of $AgNO_3$: (d) 0.05 mmol, (e) 0.10 mmol, (f) 0.25 mmol, (g) 0.50 mmol, and (d) 0.75 mmol the scale bar is 20 μm.

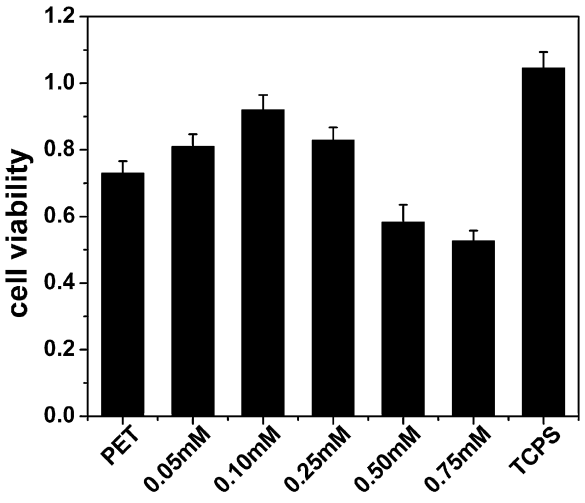

Fig. 6. The MTT assay of HUVECs cultured on pristine PET sheet, chitosan-Ag/PVP nanocomposite films and TCPS.

Especially when the $AgNO_3$ concentration was higher than 0.25 mmol, the nanocomposite films exhibited obvious cytotoxicity. Fig. 6 showed quantitative assessment of the cytotoxicity by MTT assay of cells with chitosan-Ag/PVP nanocomposite films over a period of 24 h. It could be observed that the cell viability of the HUVECs on the nanocomposite films surpassed 80% of that on TCPS when the $AgNO_3$ concentration was not higher than 0.25 mmol, which confirmed the results of FDA. The above results suggested that chitosan-Ag/PVP nanocomposite films with $AgNO_3$ concentration not higher than 0.25 mmol had low cytotoxicity and good biocompatibility. The films with 0.25 mmol $AgNO_3$ were used to investigate antibacterial properties in the following sections if without any particular explanation.

3.3. Antibacterial properties

3.3.1. Bactericidal activity test

In order to clarify the bactericidal activity of the chitosan-Ag/PVP nanocomposite film, *S. aureus* (ATCC 6538) and *E. coli* (ATCC 8739) strains were exposed to PET sheet and the nanocomposite film with the similar surface area of 14.1 cm^2 (including two sides) by shaking culture method. After 5 and 10 min exposure, the number of survived bacteria was measured by dilution-plate method. The number of bacteria did not change after contacting with PET sheets for 10 min. All of the bacteria could be eliminated in 5 min after contacting with the nanocomposite film which showed that the chitosan-Ag/PVP nanocomposite film was effective in bacteria killing. The bactericidal speed of chitosan-Ag/PVP nanocomposite film was faster than other Ag NPs loaded coatings (Cao, Liu, Meng, & Chu, 2011; Su et al., 2009). The reason could be explained in two aspects. On the one hand, chitosan exhibited bactericidal activity through contact killing or dissolving from the film. Interaction between positively charged chitosan molecules and negatively charged microbial cell membranes leads to the leakage of bacteria by disrupting the inner organelles or disturbing the metabolism of bacterial strains (Baur, Rubner, Reynolds, & Kim, 1999). On the other hand, the chitosan-Ag/PVP nanocomposite film with a thickness of 3.7 ± 0.2 μm could load massive Ag(17.43 ± 1.91 μg/cm^2)measured by ICP-MS. There was a rapid release in initial stage after immersing in PBS as indicated in the following text.

Fig. 7 shows typical antimicrobial test results of PET and chitosan-Ag/PVP nanocomposite film against *S. aureus* by agar diffusion method. It could be seen that there were many bacterial colonies around and under the PET sheet without any clear inhibition zone. While the nanocomposite film exhibited distinctive antibacterial effects against *S. aureus* with a clear zone of 3–4 mm forming around the film. These results suggested that silver ions released and diffused from the nanocomposite film which also gave a reasonable reason why there was a quick bactericidal activity of the nanocomposite film in the shaking culture test.

3.3.2. Anti-adhesion activity test

Adhesion of bacteria on medical devices is basically affected by the various chemical and physicochemical properties of the surface, among which hydrophilicity and roughness are two of the significant factors. Generally, hydrophobic surface (Serizawa, Yamaguchi, & Akashi, 2002) or rough surface (Teixeira et al., 2006) can enhance bacteria attachment as most of the proteins and bacteria are hydrophobic. As indicated in Fig. 8, the adhesion of *E. coli* on chitosan-Ag nanocomposite film was found much greater than that on chitosan-Ag/PVP coated PET sheets. Furthermore, the number of adhesive bacteria decreased with increasing content of PVP from 15 wt% to 50 wt%. Although Ag NPs and chitosan had good antibacterial property, there were still a lot of bacteria on the surface of chitosan-Ag film. The reason was mainly due to the hydrophobicity of chitosan (water contact angle: $81.5 \pm 1.2^\circ$) that made the chitosan-Ag film appropriate for bacteria adhesion. PVP as a hydrophilic polymer molecular added to the films could enhance the hydrophilicity and swelling properties of the

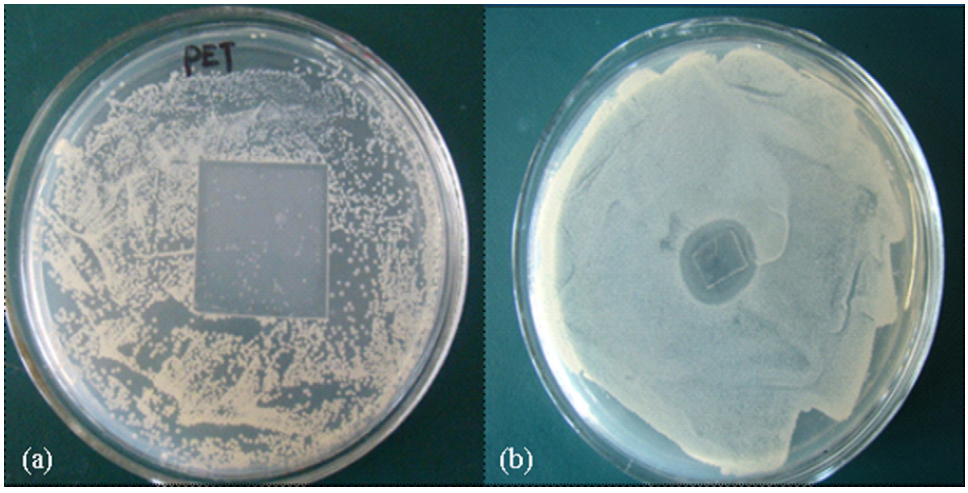

Fig. 7. Inhibition zones of (a) PET sheet and (b) chitosan-Ag/PVP (0.25 mmol $AgNO_3$) nanocomposite film coated PET against *S. aureus*.

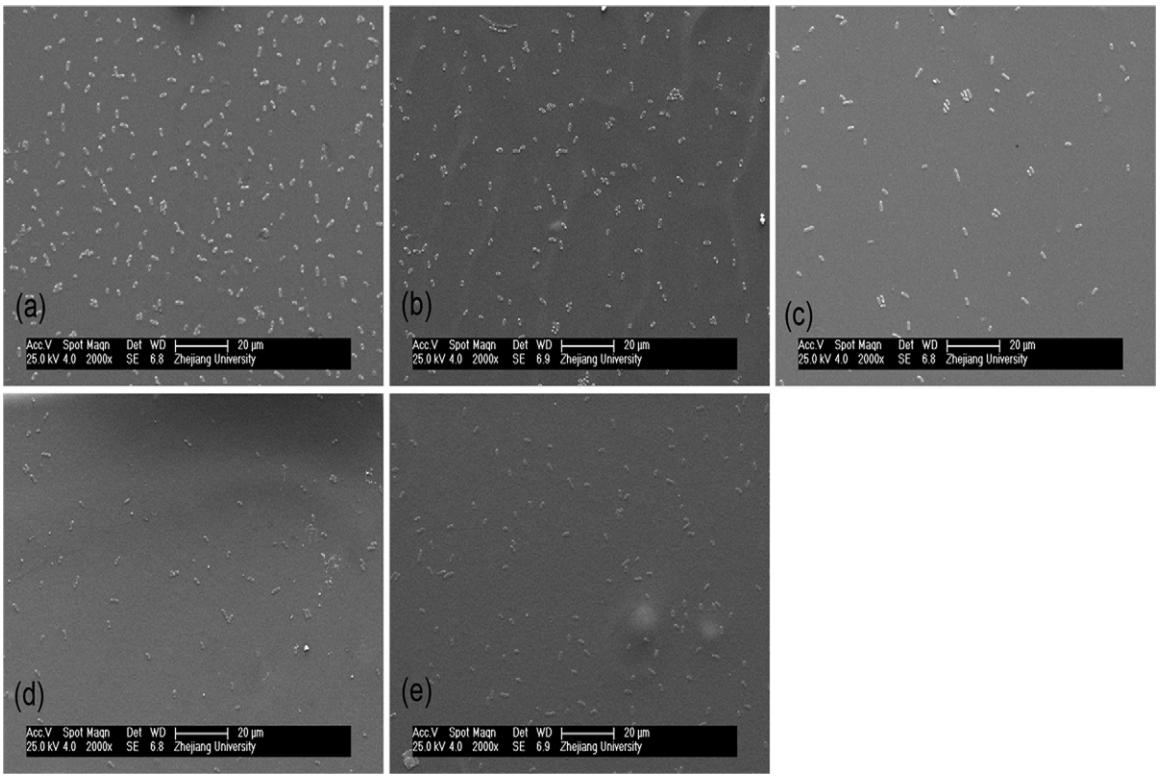

Fig. 8. SEM images of (a) chitosan-Ag and chitosan-Ag/PVP nanocomposite film (0.25 mmol $AgNO_3$) with different amounts of PVP: (b) 15 wt%, (c) 25 wt%, (d) 35 wt%, and (e) 50 wt% after exposure to waterborne *E. coli*.

films. With the increase of PVP content, static contact angle of the chitosan-Ag/PVP nanocomposite film gradually decreased from $74.2 \pm 1.4^{\circ}$ (15 wt% PVP) to $55.4 \pm 1.5^{\circ}$ (50 wt% PVP) exhibiting obvious hydrophilic property. It was demonstrated by AFM test that the chitosan-Ag/PVP nanocomposite film was smooth and flat which are beneficial to resist bacteria adhesion. However, when the amount of PVP added was higher than 25 wt%, the anti-adhesive activity of the nanocomposite films was not quite different.

3.3.3. *Long-acting bactericidal activity test*

Shaking flask culture and spread plate methods were used to investigate the long-acting bactericidal activity of the chitosan-Ag/PVP (0.25 mmol $AgNO_3$) nanocomposite film after being immersed in PBS for 35 days. The bactericidal activity of the film was strong enough to kill 100% of the *E. coli* in 30 min, which was more than 5 log cycle reduction in the number of *E. coli*. As observed in Fig. 1b, the film was stable in water with only 10% loss of thickness after 35 days immersing. Moreover, the sustained release of silver ions from the chitosan-Ag/PVP matrix could give a reasonable explanation of the long-acting bactericidal activity of the nanocomposite film. So the nanocomposite film could act as an effective bactericidal coating for a long time of 35 days.

4. Conclusion

The dip coating method has been to fabricate the Ag NPs loading chitosan-Ag/PVP nanocomposite films. Pretreatment of the substrates obviously enhanced the stability of the films. The amount and size of Ag NPs could be regulated through change the concentration of $AgNO_3$. The nanocomposite films showed fine cellular compatibility when the concentration of Ag NPs was not higher than 0.25 mmol. The anti-adhesion activity of the nanocomposite films could be obviously enhanced when the amount of PVP surpassed 25 wt%. The film exhibited fast and long-acting bactericidal activity towards *S. aureus* and *E. coli*. We believe that chitosan-Ag/PVP nanocomposite films have potential applications in the field of medical devices.

Acknowledgements

Financial supports from the the National Basic Research Program of China (2011CB606203), NSFC-50830106, 21174126, National Science Fund for Distinguished Young Scholars (51025312), Ph. D. Programs Foundation of Ministry of Education of China (20110101110037) and Open Project of State Key Laboratory of Supramolecular Structure and Materials (SKLSSM 201204) are gratefully acknowledged.

References

Anjali Devi, D., Smitha, B., Sridhar, S., & Aminabhavi, T. M. (2006). Novel crosslinked chitosan/poly(vinylpyrrolidone) blend membranes for dehydrating tetrahydrofuran by the pervaporation technique. *Journal of Membrane Science*, *280*, 45–53.

Bancel, S., & Hu, W. S. (1996). Confocal laser scanning microscopy examination of cell distribution in macroporous microcarriers. *Biotechnology Progress*, *12*, 398–402.

Baur, J. W., Rubner, M. F., Reynolds, J. R., & Kim, S. (1999). Forster energy transfer studies of polyelectrolyte hetero structures containing conjugated polymers: A means to estimate layer interpenetration. *Langmuir*, *15*, 6460–6469.

Boulmedais, F., Frisch, B., Etienne, O., Lavalle, P. H., Picart, C., Ogier, J., et al. (2004). Polyelectrolyte multilayer films with pegylated polypeptides as a new type of anti-microbial protection for biomaterials. *Biomaterials*, *25*, 2003–2011.

Bratskaya, S., Marinin, D., Simon, F., Synytska, A., Zschoche, S., & Busscher, H. J. (2007). Adhesion and viability of two Enterococcal strains on covalently grafted chitosan and chitosan/(-carrageenan multilayers. *Biomacromolecules*, *8*(9), 2960–2968.

Cao, H. L., Liu, X. Y., Meng, F. H., & Chu, P. K. (2011). Biological actions of silver nanoparticles embedded in titanium controlled by micro-galvanic effects. *Biomaterials*, *32*, 693–705.

Cao, S. G., Shi, Y. Q., & Chen, G. W. (1998). Blend of chitosan acetate salt with poly(N-vinyl-2-pyrrolidone): Interaction between chain–chain. *Polymer Bulletin*, *41*, 553–559.

Chen, S. P., Wu, G., & Zeng, H. (2005). Preparation of high antimicrobial activity thiourea chitosan–Ag^{+} complex. *Carbohydrate Polymers*, *60*, 33–38.

Clemenson, S., David, L., & Espuche, E. (2007). Structure and morphology of nanocomposite films prepared from polyvinyl alcohol and silver nitrate: Influence of thermal treatment. *Journal of Polymer Science A: Polymer Chemistry*, *45*(13), 2657–2672.

El-Rafie, M. H., Mohamed, A. A., Shaheen, T. I., & Hebeish, A. (2010). Antimicrobial effect of silver nanoparticles produced by fungal process on cotton fabrics. *Carbohydrate Polymers*, *80*, 779–782.

Fu, J. H., Ji, J., Fan, D. Z., & Shen, J. C. (2006). Construction of antibacterial multilayer films containing nanosilver via layer-by-layer assembly of heparin and chitosan–silver ions complex. *Journal of Biomedical Materials Research A*, *79A*(3), 665–674.

Fu, J. H., Ji, J., Yuan, W. Y., & Shen, J. C. (2005). Construction of anti-adhesive and antibacterial multilayer films via layer-by-layer assembly of heparin and chitosan. *Biomaterials*, *26*, 6684–6692.

Han, J., Zhou, Z., Yin, R., Yang, D., & Nie, J. (2010). Alginate-chitosan/hydroxyapatite polyelectrolyte complex porous scaffolds: Preparation and characterization. *International Journal of Biological Macromolecules*, *46*, 199–205.

Kang, H. Y., Jung, M. J., & Jeong, Y. K. (2000). Antibacterial activity and the stability of Ag^{+} solution made using metallic silver. *Korean Journal of Biotechnology and Bioengineering*, *15*, 521–524.

Lala, N. L., Ramaseshan, R., Bojun, L., Sundarrajan, S., Barhate, R. S., Liu, Y. J., et al. (2007). Fabrication of nanofibers with antimicrobial functionality used as filters: Protection against bacterial contaminants. *Biotechnology and Bioengineering*, *97*(6), 1357–1365.

Li, J., Zivanovic, S., Davidson, P. M., & Kit, K. (2011). Production and characterization of thick, thin and ultra-thin chitosan/PEO films. *Carbohydrate Polymers*, *83*, 375–382.

Lichter, J. A., Van Vliet, K. J., & Rubner, M. F. (2009). Design of antibacterial surfaces and interfaces: Polyelectrolyte multilayers as a multifunctional platform. *Macromolecules*, *42*, 8573–8586.

Lord, M. S., Cheng, B., McCarthy, S. J., Jung, M. S., & Whitelock, J. M. (2011). The modulation of platelet adhesion and activation by chitosan through plasma and extracellular matrix proteins. *Biomaterials*, *32*, 6655–6662.

Mahltig, B., Gutmann, E., Meyer, D. C., Reibold, M., Bund, A., & BÖttcher, H. (2009). Thermal preparation and stabilization of crystalline silver particles in SiO_2-based coating solutions. *Journal of Sol–Gel Science and Technology*, *49*(2), 202–208.

Muzzarelli, R. A. A., Boudrant, J., Meyer, D., Manno, N., DeMarchis, M., & Paoletti, M. G. (2012). Current views on fungal chitin/chitosan, human chitinases, food preservation, glucans, pectins and inulin: A tribute to Henri Braconnot, precursor of the carbohydrate polymers science on the chitin bicentennial. *Carbohydrate Polymers*, *87*, 995–1012.

Muzzarelli, R. A. A., Tarsi, R., Filippini, O., Giovanetti, E., Biagini, G., & Varaldo, P. E. (1990). Antimicrobial properties of N-carboxybutyl chitosan. *Antimicrobial Agents and Chemotherapy*, *34*, 2019–2023.

Picart, C., Schneider, A., Etienne, O., Mutterer, J., Schaaf, P., Egles, C., et al. (2005). Controlled degradability of polysaccharide multilayer films in vitro and in vivo. *Advanced Functional Materials*, *15*(11), 1771–1780.

Rhim, J. W., Hong, S. I., Park, H. M., & Perry, K. W. N. (2006). Preparation and characterization of chitosan-based nanocomposite films with antimicrobial activity. *Journal of Agriultural & Food Chemistry*, *54*, 5814–5822.

Richert, L., Boulmedais, F., Lavalle, P., Mutterer, J., Ferreux, E., & Picart, C. (2004). Improvement of stability and cell adhesion properties of polyelectrolyte multilayer films by chemical cross-linking. *Biomacromolecules*, *5*(2), 284–294.

Sakurai, K., Maegawa, T., & Takahashi, T. (2000). Glass transition temperature of chitosan and miscibility of chitosan/poly(N-vinyl pyrrolidone) blends. *Polymer*, *41*, 7051–7056.

Serizawa, T., Yamaguchi, M., & Akashi, M. (2002). Alternating bioactivity of polymeric layer-by-layer assemblies: Anticoagulation vs procoagulation of human blood. *Biomacromolecules*, *3*, 724–731.

Smitha, B., Sridhar, S., & Khan, A. A. (2006). Chitosan-poly(vinyl pyrrolidone) blends as membrane for direct methanol fuel cell applications. *Journal of Power Sources*, *159*, 846–854.

Su, H. L., Chou, C. C., Hung, D. J., Lin, S. H., Pao, I. C., & Lin, J. H. (2009). The disruption of bacterial membrane integrity through ROS generation induced by nanohybrids of silver and clay. *Biomaterials*, *30*, 5979–5987.

Susumu, K., Uyeda, H. T., Medintz, I. L., Pons, T., Delehanty, J. B., & Mattoussi, H. (2007). Enhancing the stability and biological functionalities of quantum dots via compact multifunctional ligands. *Journal of the American Chemical Society*, *129*(45), 13987–13996.

Teixeira, R., Trindade, A. C., Godinho, M. H., Azeredo, J., Oliveira, R., & Fonseca, J. G. (2006). *Staphylococcus epidermidis* adhesion on modified urea/urethane elastomers. *Journal of Biomaterials Science, Polymer Edition*, *17*(1–2), 239–246.

Tolaymat, T. M., El Badawy, A. M., Genaidy, A., Scheckel, K. G., Luxton, T. P., & Suidan, M. (2010). An evidence-based environmental perspective of manufactured silver nanoparticle in syntheses and applications: A systematic review and critical appraisal of peer-reviewed scientific papers. *Science of the Total Environment*, *408*, 999–1006.

Yamane, S., Iwasaki, N., Majima, T., Funakoshi, T., Masuko, T., & Harada, K. (2005). Feasibility of chitosan-based hyaluronic acid hybrid biomaterial for a novel scaffold in cartilage tissue engineering. *Biomaterials*, *26*, 611–619.

Yang, H. C., Wang, W. H., Huang, K. S., & Hon, M. H. (2010). Preparation and application of nanochitosan to finishing treatment with anti-microbial and anti-shrinking properties. *Carbohydrate Polymers*, *79*, 176–179.